Sheffield Hallam University

Atomic data from the IRON Project. I. Electron-impact scattering of Fe17+ using <I>R</I>-matrix theory with intermediate coupling

WITTHOEFT, M. C., BADNELL, N. R., BERRINGTON, K. A., PELAN, J. C. and ZANNA, G. del

This document is the

Citation:

Copyright and re-use policy

Atomic Data from the IRON Project

I. Electron-impact scattering of Fe^{17+} using R-matrix theory with intermediate coupling

M. C. Witthoeft[1], N. R. Badnell[1], K. A. Berrington[2], J. C. Pelan, and G. del Zanna[3]

[1] Department of Physics, University of Strathclyde, Glasgow G4 0NG, UK
[2] School of Science and Mathematics, Sheffield Hallam University, Sheffield, S1 1WB, UK
[3] Department of Applied Mathematics and Theoretical Physics, The Centre for Mathematical Sciences, Wilberforce Road, Cambridge CB3 0WA, Cambridge, UK

Abstract. We present results for electron-impact excitation of F-like Fe calculated using R-matrix theory with an intermediate-coupling frame transformation (ICFT) to obtain level-resolved collision strengths. Two such calculations are performed, the first expands the target using $2p^5$, $2s2p^6$, $2p^43l$, $2s2p^53l$, and $2p^63l$ configurations while the second calculation includes the $2p^44l$, $2s2p^54l$, and $2p^64l$ configurations as well. The effect of the additional structure in the latter calculation on the $n = 3$ resonances is explored and emission of a low density Fe^{17+} plasma is modeled using ADAS to explore the net effect of the differences.

1. Introduction

This work is a continuation of research done as part of the IRON Project (Hummer et al., 1993) whose goal is to provide accurate atomic data for astrophysically relevant elements using the most sophisticated computational methods to date. The focus of this work is the calculation of all fine-structure collision strengths of electron-impact excitation of Fe^{17+} for single-promotion transitions from the ground level up to the $n = 4$ levels and all transitions between them. An investigation is made examining the difference between this calculation and a smaller calculation which only considers excited states with $n \leq 3$. These studies consist of direct comparisons of collision strengths and effective collision strengths as well as emission spectra from the ADAS suite of collisional-radiative modeling codes (http://adas.phys.strath.ac.uk).

Previous works on this ion consist of distorted wave calculations by Mann (1983) and Cornille et al. (1992), a relativistic distorted wave of Sampson et al. (1991), and a non-relativistic R-matrix calculation of Mohan et al. (1987) which included the $2s^22p^5$, $2s2p^6$, and $2s^22p^43l$ terms. A previous IRON Project report, IP XXVIII (Berrington et al., 1998), examined, using R-matrix theory, just the fine structure transition of the ground term, $^2P_{3/2} \rightarrow\ ^2P_{1/2}$, for several F-like ions including Fe using the same target expansion as the present ($n = 3$)-state calculation.

The rest of this paper is organized as follows. In Sec. II, the details of the present calculations will be discussed including a comparison of our target structure with other calculations and experimental results. In Sec. III, the results of both R-matrix calculations are presented and discussed. Finally, in Sec. IV, we provide a brief conclusion.

2. Calculation

As mentioned before, two R-matrix calculations are performed for this report. The intermediate-coupling frame transformation (ICFT) method of Griffin et al. (1998) using multi-channel quantum defect theory (MQDT) is utilized to enable us to perform much of the calculation in LS coupling. The advantage of this approach is realized in the diagonalization time of the $(N + 1)$-electron Hamiltonian whose size is determined by the number of LS terms and not the larger number of jK levels. In the smaller (n=3)-state calculation we include the $2s^22p^5$, $2s2p^6$, $2s^22p^43l$, $2s2p^53l$, and $2p^63l$ terms; a total of 52 terms containing 113 fine-structure levels. The second calculation is an extension of the first adding the $2s^22p^44l$, $2s2p^54l$, and $2p^64l$ terms to the target expansion. This results in a total of 124 terms and 279 levels.

The target structure and resulting wave functions are calculated using AUTOSTRUCTURE (see Badnell, 1986) where a radial scaling parameter, λ_{nl}, of each orbital is varied to minimize the average energy of each term. The radial scaling parameters used for both calculations are

Table 1. Radial scaling factors used in AUTOSTRUCTURE to minimize the total energy of the nl orbital wave functions.

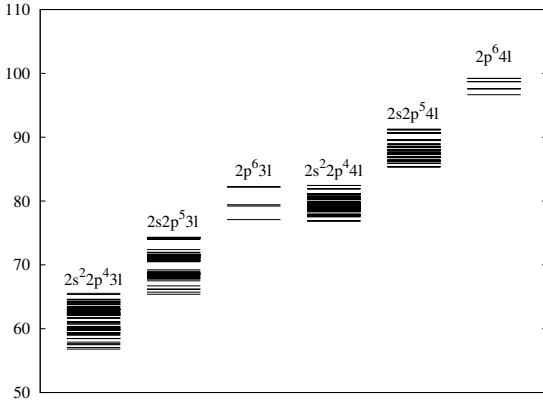|	$n = 3$	$n = 4$
λ_{1s}	1.3895	1.3923
λ_{2s}	1.1971	1.2076
λ_{2p}	1.1313	1.1404
λ_{3s}	1.1315	1.1266
λ_{3p}	1.0857	1.0807
λ_{3d}	1.1223	1.1122
λ_{4s}	-	1.1219
λ_{4p}	-	1.0807
λ_{4d}	-	1.1077
λ_{4f}	-	1.1133

Fig. 1. Energy levels in Ry for both the $n = 3$ (left) and $n = 4$ (right) structure calculations from AUTOSTRUCTURE.

given in Table I. The $n = 3$ energy levels are not changed significantly by the addition of the $n = 4$ levels in the larger calculation. The reason for this is demonstrated in Figure 1 where the energy levels for the $n = 4$ calculation are displayed. The only overlap between the $n = 3$ and $n = 4$ levels is between the $2p^63l$ and $2s^22p^44l$ levels. Since only two-electron transitions connect these levels, this overlap does not have a significant effect on the energy levels. In Table II are listed the energies of the lowest 66 levels from the $n = 4$ calculation compared to those listed on the NIST website (Corliss & Sugar, 1982; http://physics.nist.gov). Since the level energies of the $n = 3$ calculation are within 0.1% of the $n = 4$ calculation they are not shown. With the exception of the first two excited states, which disagree by 2% and 1% respectively, all our level energies agree with the measurements of Corliss & Sugar to within 0.5%. We shall subsequently refer to levels using the energy ordered index given in this table.

As a final test of the structure, we compare our oscillator strengths with previous calculations. In Table III are listed the oscillator strengths for both our $n = 3$ and $n = 4$-state calculations with a SUPERSTRUCTURE calculation of Cornille et al. (1992) and the relativistic atomic structure calculation by Sampson et al. (1991). There is generally good agreement between all the calculations.

Both the $n = 3$ and $n = 4$ R-matrix calculations include the mass-velocity and Darwin corrections and include a total of 20 continuum terms per channel. A full-exchange calculation is performed for $J \leq 10$ and a non-exchange calculation then provides the contribution up to $J = 38$ and a further top-up is done using the Burgess sum rule (see Burgess, 1974). In the outer region, we calculate the collision strengths up to an electron-impact energy of 200 Ry on a energy mesh with a spacing of $10^{-5}z^2$ Ry in regions with strong resonance contributions, a spacing of $10^{-4}z^2$ Ry was used for the region between the $n = 2$ and $n = 3$ resonances, and a spacing of $10^{-3}z^2$ Ry was used for high energies outside the resonance region. Although this energy spacing does not resolve all resonances, the more than 15 000 energy points used are believed to to sufficiently sample the small width resonances as discussed by Badnell & Griffin (2001).

Effective collision strengths at high temperatures are obtained for dipole and Born allowed transitions by interpolation between the R-matrix calculation at 200 Ry and an infinte energy point calculated by AUTOSTRUCTURE.

3. Results

Overall, the differences between the $n = 3$ and $n = 4$ calculations are small. In Fig. 2, we compare the collision strength of both calculations for the 1-4 transition. While the $n = 3$ calculation shows stronger resonant enhancement for scattered electron energies below 3 Ry, the differences are not excessive. We also observe that the additional $n = 4$ resonances for energies larger than 10 Ry are small and not likely to have a large effect on the effective collision strength. Similar features are seen for the 2-4 transition in Fig. 3.

To get a better measure of the resonant enhancement, we plot in Figures 4 and 5 the effective collision strengths for the 1-4 and 2-4 transitions respectively. Also included in these figures is a reduced $n = 3$ R-matrix calculation by Mohan et al. (1987) where the $2s2p^53l$ and $2p^63l$ terms are not included in the target expansion. In Fig. 4, there is about a 10% difference between the present $n = 3$ and $n = 4$ calculations while the Mohan et al. calculation is a factor of four smaller at low temperatures and only coming within a factor of two at the highest temperatures shown. We see a similar disagreement between the Mohan et al. results and the present calculation in Fig. 5 for the 2-4 transition. In this case, however, the collision strength of the $n = 4$ calculation is about 50% higher than that of the $n = 3$ calculation at low temperatures, although the absolute difference for this weak transition is about the same as in the 1-4 transition. Again, the effective collision strength from the Mohan et al. calculation is much smaller at low temperatures and coming into decent agreement at the end of the plotted temperature range. The difference between the Mohan et al. calculation and our $n = 3$ calculation demonstrates the importance of the $2s2p^53l$ terms on transitions involving the $2s^22p^43l$ levels.

Table 2. Lowest 66 energy levels in Ry for $n = 4$ calculation compared to experimental measurements of Corliss & Sugar (1982) (see http://physics.nist.gov).

i	Level	Present	NIST	i	Level	Present	NIST	i	Level	Present	NIST
1	$2p^5\ ^2P^o_{3/2}$	0.0	0.0	23	$2p^43p\ ^2S^o_{1/2}$	60.309		45	$2p^43d\ ^4F_{7/2}$	63.111	
2	$2p^5\ ^2P^o_{1/2}$	0.955	0.935	24	$2p^43p\ ^2D^o_{3/2}$	60.356		46	$2p^43d\ ^2D_{3/2}$	63.140	
3	$2s2p^6\ ^2S_{1/2}$	9.830	9.702	25	$2p^43p\ ^2F^o_{5/2}$	60.693		47	$2p^43d\ ^4P_{5/2}$	63.297	62.911
4	$2p^43s\ ^4P_{5/2}$	56.798	56.699	26	$2p^43p\ ^2F^o_{7/2}$	60.878		48	$2p^43d\ ^2P_{3/2}$	63.418	63.308
5	$2p^43s\ ^2P_{3/2}$	57.052	56.937	27	$2p^43p\ ^2D^o_{3/2}$	61.016		49	$2p^43d\ ^2D_{5/2}$	63.516	63.401
6	$2p^43s\ ^4P_{1/2}$	57.492	57.503	28	$2p^43p\ ^2D^o_{5/2}$	61.126		50	$2p^43d\ ^2G_{7/2}$	63.787	
7	$2p^43s\ ^4P_{3/2}$	57.664	57.573	29	$2p^43p\ ^2P^o_{3/2}$	61.590		51	$2p^43d\ ^2G_{9/2}$	63.825	
8	$2p^43s\ ^2P_{1/2}$	57.899	57.798	30	$2p^43p\ ^2P^o_{1/2}$	61.758		52	$2p^43d\ ^2F_{5/2}$	64.052	
9	$2p^43s\ ^2D_{5/2}$	58.444		31	$2p^43d\ ^4D_{5/2}$	62.114		53	$2p^43d\ ^2S_{1/2}$	64.056	63.919
10	$2p^43s\ ^2D_{3/2}$	58.478	58.355	32	$2p^43d\ ^4D_{7/2}$	62.127		54	$2p^43d\ ^2F_{7/2}$	64.156	
11	$2p^43p\ ^4P^o_{3/2}$	59.019		33	$2p^43d\ ^4D_{3/2}$	62.157		55	$2p^43d\ ^2P_{3/2}$	64.280	64.139
12	$2p^43p\ ^4P^o_{5/2}$	59.053		34	$2p^43d\ ^4D_{1/2}$	62.247		56	$2p^43d\ ^2D_{5/2}$	64.335	64.160
13	$2p^43p\ ^4P^o_{1/2}$	59.296		35	$2p^43p\ ^2P^o_{3/2}$	62.335		57	$2p^43d\ ^2D_{3/2}$	64.558	64.391
14	$2p^43p\ ^4D^o_{7/2}$	59.350		36	$2p^43d\ ^4F_{9/2}$	62.356		58	$2p^43d\ ^2P_{1/2}$	64.623	64.465
15	$2p^43p\ ^4D^o_{5/2}$	59.365		37	$2p^43d\ ^2F_{7/2}$	62.452		59	$2p^43d\ ^2D_{5/2}$	65.356	65.305
16	$2p^43s\ ^2S_{1/2}$	59.807	59.917	38	$2p^43p\ ^2P^o_{1/2}$	62.542		60	$2s2p^53s\ ^4P^o_{5/2}$	65.396	
17	$2p^43p\ ^4D^o_{1/2}$	59.810		39	$2p^43d\ ^4P_{1/2}$	62.597	62.497	61	$2p^43d\ ^2D_{3/2}$	65.542	65.468
18	$2p^43p\ ^4D^o_{3/2}$	59.840		40	$2p^43d\ ^4P_{3/2}$	62.734	62.626	62	$2s2p^53s\ ^4P^o_{3/2}$	65.726	
19	$2p^43p\ ^2P^o_{1/2}$	59.844		41	$2p^43d\ ^2F_{5/2}$	62.816		63	$2s2p^53s\ ^4P^o_{1/2}$	66.140	
20	$2p^43p\ ^2P^o_{3/2}$	59.980		42	$2p^43d\ ^2P_{1/2}$	62.957		64	$2s2p^53s\ ^2P^o_{3/2}$	66.221	
21	$2p^43p\ ^4D^o_{5/2}$	60.124		43	$2p^43d\ ^4F_{3/2}$	62.989		65	$2s2p^53s\ ^2P^o_{1/2}$	66.709	
22	$2p^43p\ ^4S^o_{3/2}$	60.157		44	$2p^43d\ ^4F_{5/2}$	63.012		66	$2s2p^53p\ ^4S_{3/2}$	67.505	

Table 3. Comparison of various calculated gf-values for present calculations with Cornille et al. (1992) and Sampson et al. (1991).

trans	$n = 3$	$n = 4$	Cornille	Sampson
1-4	0.0197	0.0198	0.020	0.0172
1-5	0.2409	0.2419	0.247	0.2184
2-5	0.0063	0.0062	0.006	0.0056
1-6	0.0136	0.0136	0.010	0.0136
2-6	0.0004	0.0004		0.0004
1-10	0.0023	0.0024	0.003	0.0024
2-10	0.1789	0.1818	0.185	0.1646
1-43	0.0892	0.0887	0.057	0.0912
2-43	0.0093	0.0094	0.009	0.0108
1-58	0.2826	0.2683	0.284	0.2968
2-58	1.383	1.356	1.40	1.294

The 1-4 and 2-4 transition comparisons are typical of the rest of the transitions with few exceptions. In some cases, particularly for very weak transitions, the $n = 4$ resonant enhancement can dominate over the $n = 3$ resonances. To illustrate this scenario, we show, in Fig. 6, a comparison of the 2-66 collision strength for both calculations Here we see, not only the strong, extended $n = 4$ resonant features in the larger calculation, but the $n = 4$ calculation also has much stronger enhancement of the $n = 3$ resonance contribution. Although not shown, the $n = 4$ effective collision strength is a factor of 3 larger than the $n = 3$ calculation at $\log T = 6.2$ and is twice as large for $\log T = 7.0$.

Using the ADAS suite of collisional-radiative modeling codes, we now explore how the differences seen between the two calculations effect the prediction of observed radiative emission of a low density Fe^{17+} plasma. At an electron temperature of 550 eV, the primary and secondary emission peaks are at 14.2 and 16.0 Å respectively. Both of these peaks are due to $n = 3$ levels exclusively. The largest emission peak in the region where there are both $n = 3$ and $n = 4$ levels, occurring at 13.4 Å, is 15 times smaller than the primary peak. In Figures 7, 8 and 9, we show the emission spectra for these three peaks. In addition to the spectra for the present calculations, we show the spectrum from a modified $n = 4$ plane-wave Born calculation and a hybrid spectrum which supplements the present $n = 3$ R-matrix with the $n = 4$ data from the modified plane-wave Born calculation. The modified plane-wave Born calculation is a standard plane-wave Born calculation (Burgess et al., 1997) which has been modified as to have a non-zero collision strength at threshold (see Cowan, p. 569). Starting with the primary peak in Fig. 7, we see that the peak from the $n = 4$ calculation is about 25% smaller than for the $n = 3$ calculation. The $n = 4$ modified plane-wave Born calculation severely overestimates the present $n = 4$ calculation and the hybrid result closely matches the $n = 3$ R-matrix calculation. In Fig. 8, we find that the $n = 4$ peak is larger by about 35% over the $n = 3$ peak. Again, the modified plane-wave Born calculation misses the mark having only half the intensity of the $n = 4$ R-matrix result. The hybrid result is found to improve slightly over the $n = 3$ R-matrix calculation but is still 15% lower than the $n = 4$ spectra. Finally, in Fig. 9, we examine the largest peak in the region where both the $n = 3$ and $n = 4$ resonances play a role. In this region, the
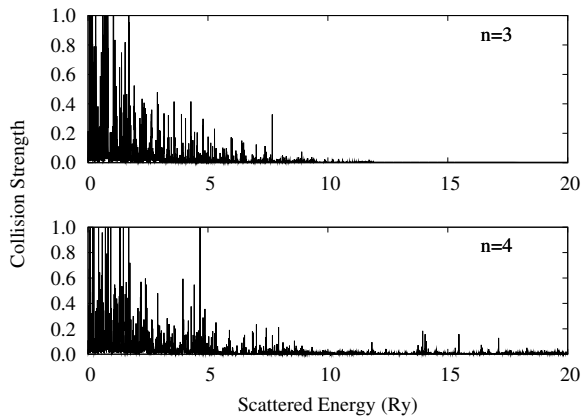
Fig. 2. Collision strengths versus scattered electron energy for the $n = 3$ (top) and $n = 4$ (bottom) calculations of the 1-4 transition.
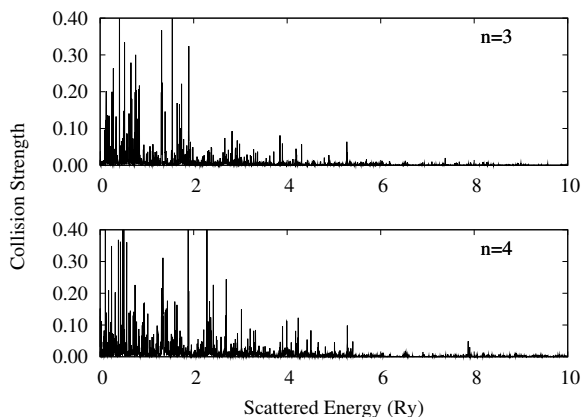

Fig. 3. Collision strengths versus scattered electron energy for the $n = 3$ (top) and $n = 4$ (bottom) calculations of the 2-4 transition.

Fig. 4. Effective collision strengths of the 1-4 transition comparing the present $n = 3$ calculation (solid), $n = 4$ calculation (dashed) and an $n = 3$ R-matrix calculation by Mohan et al. (1987).
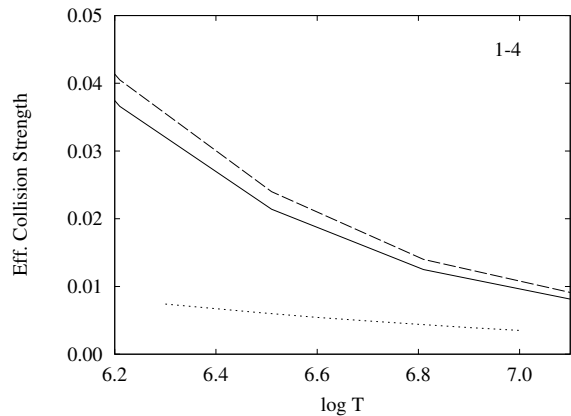

Fig. 5. Effective collision strengths of the 2-4 transition comparing the present $n = 3$ calculation (solid), $n = 4$ calculation (dashed) and an $n = 3$ R-matrix calculation by Mohan et al. (1987).
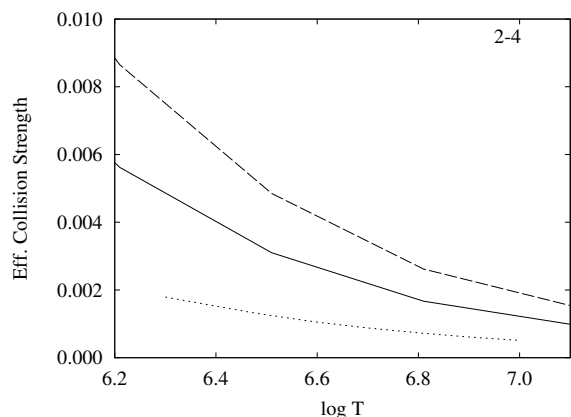
hybrid spectrum does a good job reproducing the $n = 4$ R-matrix spectrum. The modified plane-wave Born calculation is too high while the $n = 3$ R-matrix calculation is smaller than the $n = 4$ calculation. Taking all these results into account, it appears that although the $n = 4$ plane-wave Born is a poor approximation for these spectra at all wavelengths, the smaller $n = 3$ R-matrix calculation supplemented by the $n = 4$ Born calculation does perform well in the region where both $n = 3$ and $n = 4$ resonances exist and does no worse than the $n = 3$ R-matrix calculation alone where there is only emission from the $n = 3$ resonances. By extension, we would expect similar results from a hybrid data set composed of the $n = 4$ R-matrix calculation and an $n = 5$ modified plane-wave Born calculation, although this would need to be investigated.

4. Summary

Two R-matrix calculations in intermediate coupling were performed for electron-impact exctitation of Fe^{17+}. The effective collision strengths of the $n = 4$ calculation have been archived for all $38\,781$ transitions, expanding on

the work done in IP XXVIII (Berrington et al., 1998). Differences of 10-20% in the effective collision strengths between the smaller $n = 3$ calculation and the extended $n = 4$ calculation persist for the majority of the transitions. The addition of the $2s2p^53l$ and $2p^63l$ terms in the present $n = 3$ R-matrix calculation are found to have significant effects on the collision strengths to the $2s^22p^43l$ levels when compared the the R-matrix calculation of Mohan et al. (1987). The ADAS suite of collisional radiative modeling codes were used to obtain spectra from a low-density Fe^{17+} plasma at an electron temperature of 550 eV. The differences found in the collision strengths between the two R-matrix calculations translate to the intensity peaks of the emission spectra. The spectrum from a modified plane-wave Born calculation performs poorly at all wavelengths investigated but a hybrid spectrum composed of the $n = 3$ R-matrix calculation supplemented by the $n = 4$ modified plane-wave Born calculation is found to slightly improve over the $n = 3$ R-matrix calculation
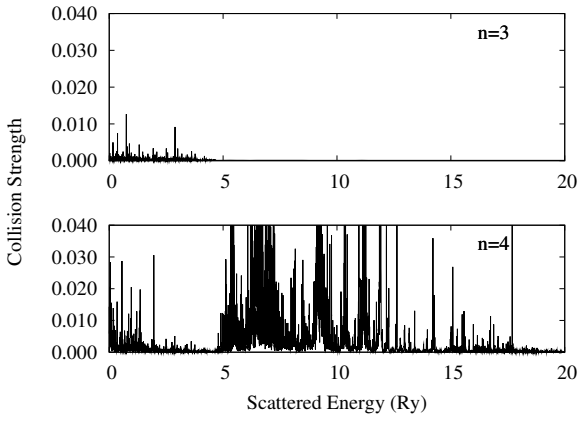
Fig. 6. Collision strengths versus scattered electron energy for the $n = 3$ (top) and $n = 4$ (bottom) calculations of the 2-66 transition.
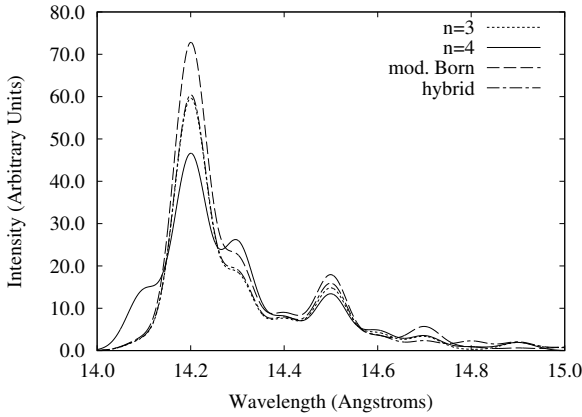

Fig. 7. Radiative emission from a collisional radiative model (ADAS) in the low denisty limit at an electron temperature of 550 eV for a wavelength range of 14.0 to 14.6 Å. The $n = 3$ calculation is the dotted curve, $n = 4$ is the solid curve, the dashed curve shows the modified plane-wave Born calculation from AUTOSTRUCTURE, and the hybrid R-matrix/Born result is shown as the dot-dash curve.

alone, especially in regions where both $n = 3$ and $n = 4$ resonances contribute.

Fig. 8. Radiative emission from a collisional radiative model (ADAS) in the low denisty limit at an electron temperature of 550 eV for a wavelength range of 15.5 to 16.4 Å. The $n = 3$ calculation is the dotted curve, $n = 4$ is the solid curve, the dashed curve shows the modified plane-wave Born calculation from AUTOSTRUCTURE, and the hybrid R-matrix/Born result is shown as the dot-dash curve.

Fig. 9. Radiative emission from a collisional radiative model (ADAS) in the low denisty limit at an electron temperature of 550 eV for a wavelength range of 12.5 to 14.0 Å. The $n = 3$ calculation is the dotted curve, $n = 4$ is the solid curve, the dashed curve shows the modified plane-wave Born calculation from AUTOSTRUCTURE, and the hybrid R-matrix/Born result is shown as the dot-dash curve.

References

ADAS web page: http://adas.phys.strath.ac.uk

Badnell, N. R. 1986, J. Phys. B: At. Mol. Phys., 19, 3827

Badnell, N. R. & Griffin, D. C. 2001, J. Phys. B: At. Mol. Opt. Phys., 34, 681

Berrington, K. A., Saraph, H. E., Tully, J. A. 1998, A&AS, 129, 161 (IP XXVIII)

Burgess, A. 1974, J. Phys. B: At. Mol. Phys., 7, L364

Burgess, A., Chidichimo, M. C., Tully, J. A. 1997 J. Phys. B: At. Mol. Opt. Phys., 30, 33

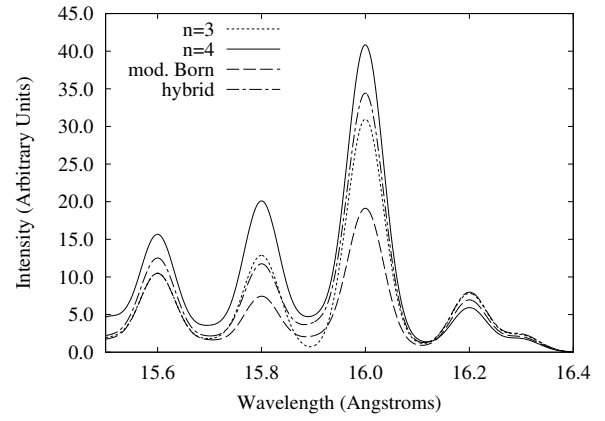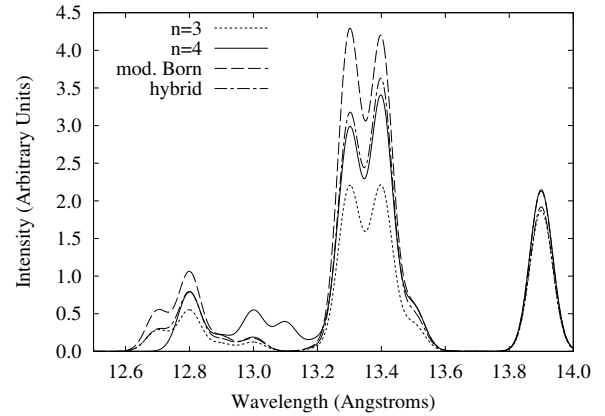Corliss, C. & Sugar, J. 1982, J. Phys. Chem. Ref. Data, 11, 135

Cornille, M., Dubau, J., Loulergue, M., Bely-Dubau, F., Faucher, P. 1992, A&A, 259, 669

Cowan, R. D. 1981, The Theory of Atomic Structure and Spectra, (California: University of California Press), 569

Griffin, D. C., Badnell, N. R., Pindzola, M. S. 1998 J. Phys. B: At. Mol. Opt. Phys., 31, 3713

Hummer, D. G., Berrington, K. A., Eissner, W., et al. 1993, A&A, 279, 298

Mann, J. B. 1983, At. Data Nuc. Data Tables, 29, 407

Mohan, M., Baluja, K. L., Hibbert, A., Berrington, K. A. 1987, J. Phys. B: At. Mol. Phys., 20, 6319

NIST web page: http://physics.nist.gov

Sampson, D. H., Zhang, H. L., Fontes, C. J. 1991, At. Data Nuc. Data Tables, 48, 25